

# EFFECTS OF HYBRID TECHNOLOGY, ULTRASONIC EDM ON SURFACE QUALITY AND ECONOMIC EVALUATION MODEL

Liviu Daniel Ghiculescu<sup>1</sup>, Anca-Valentina Duca<sup>1</sup>, Viorica Răscol<sup>1</sup>, and Roxana Silvia Ionescu<sup>1</sup>

<sup>1</sup> Department of Manufacturing Engineering, National University of Science and Technology, "Politehnica", Bucharest, Romania

**ABSTRACT:** The paper deals with a comparative study of superficial layer of CoCr alloys obtained at classic and ultrasonic (US) aided electrical discharge machining (EDM). The machined materials characteristics, the equipment used at laboratory experiments, the working values and the most relevant images of superficial layer provided by scanning electron microscope are presented. Comparative numerical simulation of discharges in case of EDM and EDM+US and their effect on the superficial layer were validated by experimental data. An economic model for evaluation of EDM+US performances was elaborated.

**KEYWORDS:** superficial layer, EDM, ultrasonic, numerical simulation

## 1. INTRODUCTION

Considering the challenges brought by advanced technologies, electrical discharge machining (EDM) is one of the best alternatives for processing an increasing number of conductive materials with high hardness, non-corrosive and wear-resistant properties [1, 2]. EDM with electrode vibration normal to the processed surface at ultrasonic frequency is characterized by a significant improvement in the main EDM parameters - increased productivity, reduced relative volumetric wear, roughness of the processed surface and the melted and resolidified surface layer [3].

## 2. THE CURRENT STAGE REGARDING THE SUPERFICIAL LAYER RESULTING FROM EDM

Surface quality involves both roughness and the structure of the surface layer affected by EDM, namely the thermal influence area. The structure of the surface layer is represented by the austenitic layer, the martensitic layer, the white layer, and the melted and resolidified metal layer - Fig. 1 [4].

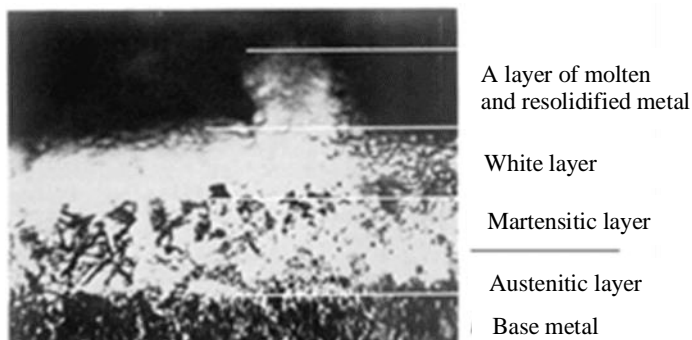


**Figure 1.** Surface layer structure, EDM [4]

Following an electrical discharge, a crater is formed. The material remaining in the craters resolidifies and is called the white layer because it has this color when

viewed under a microscope. It is not chemically attacked by usual agents (e.g. nital) [5].

It exhibits numerous micro-cracks as a result of exceeding the rupture strength caused by the thermal shock generated by discharges (see Fig. 5). Further down, a high surface hardness martensitic layer is encountered (about 1000 HV at a depth of 25  $\mu\text{m}$ ) followed by an austenitic layer, typical hardening constituents resulting from the rapid heating and cooling process of EDM. Ultrasonic (US) combination with EDM finishing (EDM+US) -*hybrid machining*, significantly reduces the white layer and hence internal stresses (by about 50%), increasing fatigue resistance (2...6 times) [4].

## 3. CHARACTERISTICS OF PROCESSED COCR ALLOYS AND EQUIPMENT USED

In general, Co-Cr alloys can be described as alloys with high wear and temperature resistance, non-magnetic, with excellent biocompatibility, corrosion resistance, and a high elastic modulus, which also ensures appropriate rigidity [6]. The chemical composition of the two alloys chosen for the study, named System NE and System SOFT, is presented in Table 1, and the mechanical characteristics that influence the layer of solid material removed by US are shown in Table 2.\_

Figure 1 shows the working head of the EDM ELER 01 machine, located in the laboratory of the FIIR faculty, TCM department, UPB, on which an ultrasonic chain was mounted, with a copper disc electrode-tool at the end.

The cylindrical-shaped samples of the two alloys were machined at one end using conventional EDM and at the other end using EDM in an ultrasonic field, in order to observe and compare the resulting surface layer obtained using the two methods - see Figure 2.

**Table 1.** Chemical composition of CoCr alloys [7]

| Alloy           | Cr [%] | Mo [%] | W [%] | Nb [%] | Si [%] | Mn [%] | Fe [%] | Co [%] |
|-----------------|--------|--------|-------|--------|--------|--------|--------|--------|
| P1, SYSTEM NE   | 21,0   | 6,5    | 6,4   | -      | 0,8    | 0,65   | <0,1   | 64,4   |
| P2, SYSTEM SOFT | 29,5   | 5,7    | -     | -      | 0,95   | 0,55   | 0,75   | 61,8   |

**Table 2.** Mechanical characteristics of CoCr alloys [7]

| Alloy           | Ultimate tensile strength [MPa] | Young modulus [GPa] | Yield strength [MPa] | Break elongation [%] | Rigidity [HV] |
|-----------------|---------------------------------|---------------------|----------------------|----------------------|---------------|
| P1, SYSTEM NE   | 850                             | 155                 | 580                  | 3                    | 460           |
| P2, SYSTEM SOFT | 447                             | 160                 | 450                  | 15                   | 310           |

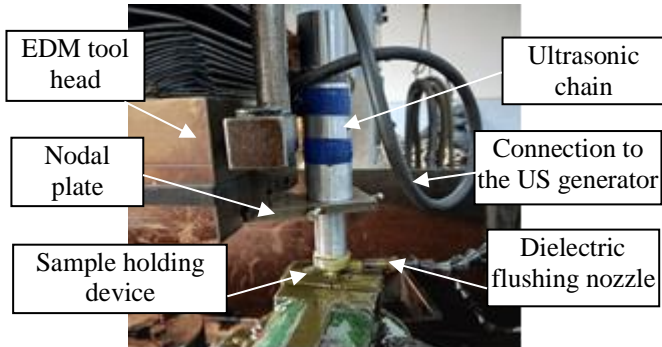


**Figure 2.** The tool head of the ELER 01 machine and the US chain mounted on it

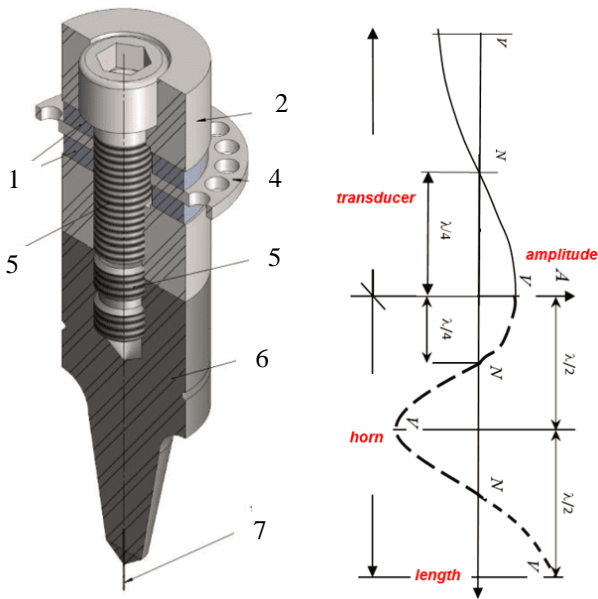


**Figure 3.** Ultrasonic chain and standing waves formed within it left – ultrasonic chain structure; right -standing waves [3]

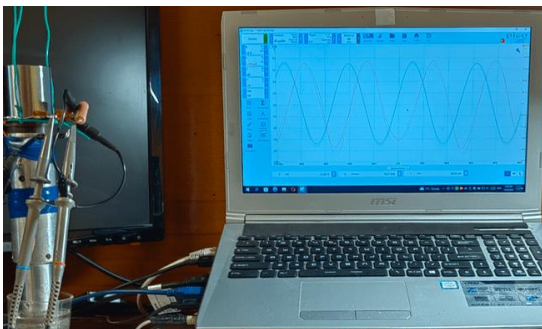


**Figure 4.** Determination of the natural frequency ( $f_0=19.21$  kHz) of the ultrasonic chain and adjustment of the generator at resonance

The US chain, fig. 3. left, presents a transducer with piezoceramic plates 1 that change their dimensions, connected in a variable electric field given by a US generator, transmitting the vibrations, standing waves, fig. 3. right along the US chain. The transducer also includes the reflecting bushing (2), nodal flange (4) for connection to the US generator, the radiating bushing (3) and the screw (5) that assembles the pre-stressed transducer components with 8-10 tf. The amplification of US oscillations is achieved through horn 6, at the end of which the micro-tool 7 is located (positioned in the antinode). The natural frequency,  $f_0=19.21$  kHz, of the US chain was determined and the US generator was adjusted to the same frequency to obtain resonance - fig. 4.

#### 4. EXPERIMENTAL DATA REGARDING THE OBTAINED SURFACE LAYER

The distribution of chemical elements in the surface layer structure of the processed alloys is presented in fig. 5, System NE and fig. 6, System Soft.

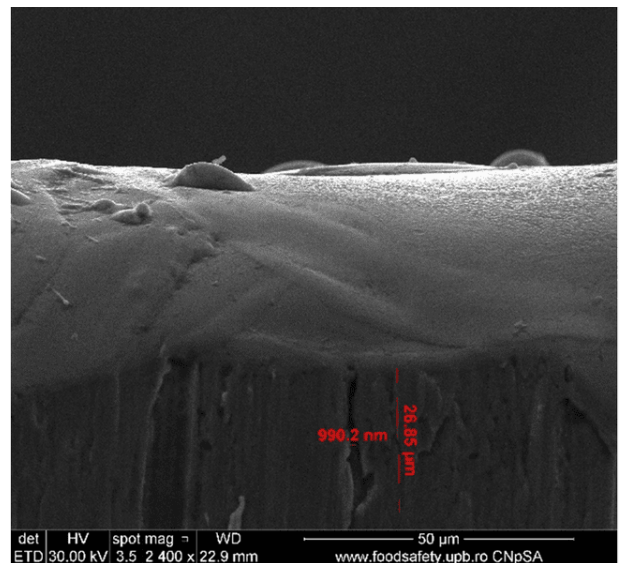
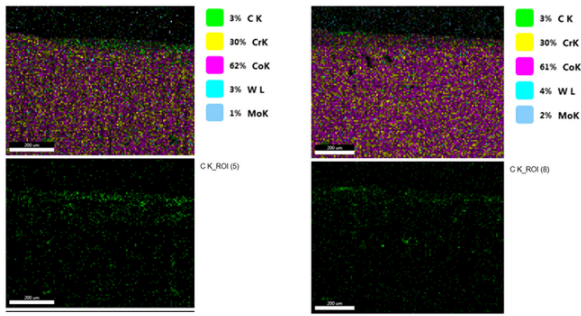


**Figure 5.** Microcrack for EDM+US System NE

This was obtained with the EDAX system, generating X-rays from samples processed by scanning with the electron beam of the SEM QUANTA INSPECT F50 - UPB microscope, with a resolution of 1 nm. A

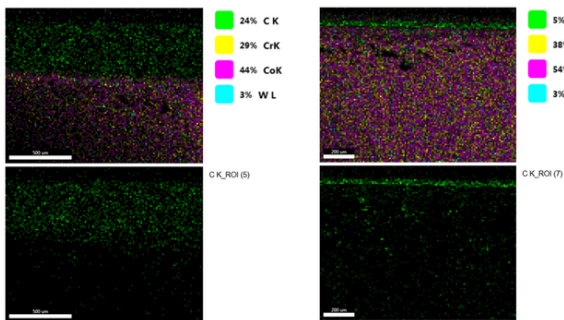
reduction in the depth of the C-enriched layer was observed due to the US effect, by collecting a larger amount of melted material by breaking the gas bubble formed around the plasma channel of the discharge at the end of a US oscillation.

Thus, for the System NE alloy, the thickness of the layer with significant C content (green color) is approximately 200  $\mu\text{m}$  for classic EDM and approximately 100  $\mu\text{m}$  for EDM+US - see the white reference point, Fig. 6; it was machined with a current  $I=12\text{ A}$  and pulse time  $t_i=95\ \mu\text{s}$ , while the power of the US generator was  $P_{us}=80\text{ W}$ .

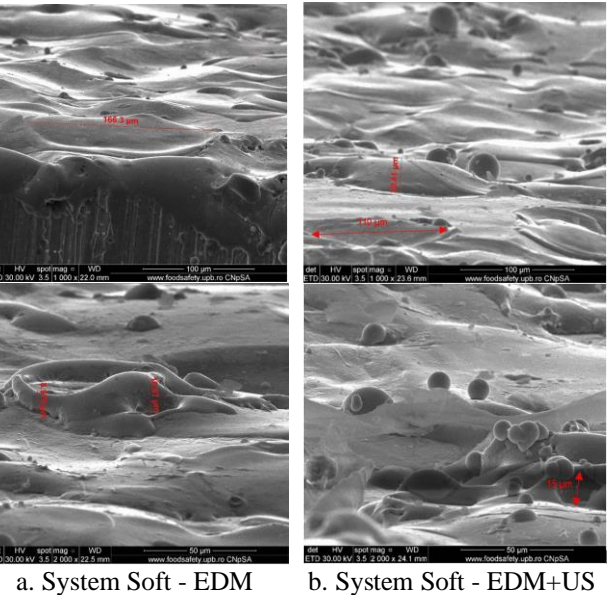
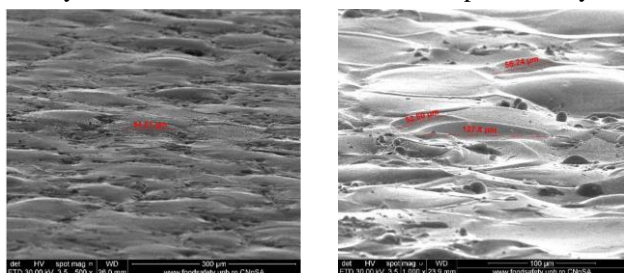


a. System NE - EDM      b. System NE - EDM+US  
**Figure 6.** Chemical elements repartition in the composition of System NE in the structure of the superficial layer

In the case of the System Soft alloy, the thickness of the layer with high C content is 500  $\mu\text{m}$  for classic EDM and approximately 50  $\mu\text{m}$  for EDM+US - see the white reference point, Fig. 7; it was machined with  $I=12\text{ A}$  and  $t_i=24\ \mu\text{s}$ ,  $P_{us}=80\text{ W}$ . This layer with microcracks, produced by the thermal shock of the EDM discharge (Fig. 5) called the white layer, is greatly reduced in the case of EDM+US.



a. System Soft - EDM      b. System Soft - EDM+US  
**Figure 7.** Chemical elements Repartition in the composition of System SOFT in the structure of the superficial layer



a. System Soft - EDM      b. System Soft - EDM+US  
**Figure 9.** Microgeometry of the machined surface at System SOFT; dimensions of craters (top) and protrusions (bottom)

The images of the microgeometry of the machined surface obtained with the same SEM microscope at the same processing parameters as before are presented comparatively in Fig. 8, 9. It can be observed that for both materials, at EDM+US compared to EDM, the dimensions of the craters are smaller, and the height of the protrusions is higher for System Soft (lower mechanical resistance to US action) compared to System NE.

## 5. NUMERIC SIMULATION OF THE CLASSIC AND ULTRASONIC ELECTRICAL DISCHARGE MACHINING

To study the material removal mechanisms in EDM+US, Comsol Multiphysics was used in 2D axisymmetric space, with the Heat Transfer in Solids module for the EDM component and the Solid Mechanics module for the US component, both time-dependent. The following steps were taken:

- (1) Parameterization of the thermal and mechanical models for both materials studied, fig. 10, 11;

| Name | Expression | Description                  | Name   | Expression                                 | Description                          |
|------|------------|------------------------------|--------|--|--------------------------------------|
| hp   | 15 [mm]    | height of the test piece     | TfCoCr | 3000                                       | Boiling temperature [C]              |
| rp   | 4[mm]      | Radius of the test piece     | TmCoCr | 1330                                       | Melting temperature [C]              |
| l    | 12         | Current step                 | rcp    | $1e-6*2.16^{*10^{0.43}}*(t^{*1e6})^{0.44}$ | Time-dependent plasma channel radius |
| tif  | 95e-6      | Final pulse time             | ti     | 0  | Sweep pulse time                     |
| acr  | 47e-6      | Initial crater radius        | a      | 1e-6                                       | Initial plasma channel radius        |
| bcr  | 4*Ra       | Initial crater depth         | tus    | 1e-6                                       | US application time                  |
| rms  | 0.8e-6     | Resolidified material radius | pus    | 120[Mpa]                                   | Ultrasonic pressure                  |
| rbg  | 0.1[mm]    | Gas bubble radius            | sigmar | 850[Mpa]                                   | Static tensile strength NE           |
| Ra   | 5.5e-6     | Ra of the processed surface  | tau0   | 211.2                                      | Shear fatigue strength NE            |

Figure 10. Model parameters System NE

| Name | Expression | Value      | Description                  | Name   | Expression                              | Description                          |
|------|------------|------------|------------------------------|--------|---|--------------------------------------|
| hp   | 15 [mm]    | 0.015 [mm] | height of the test piece     | TfCoCr | 3000                                    | Boiling temperature [C]              |
| rp   | 4[mm]      | 0.004[mm]  | Radius of the test piece     | TmCoCr | 1330                                    | Melting temperature [C]              |
| l    | 12         | 12         | Current step                 | rcp    | $1e-6*2^{*10^{0.43}}*(t^{*1e6})^{0.44}$ | Time-dependent plasma channel radius |
| tif  | 24e-6      | 2.4E-5     | Final pulse time             | ti     | 0                                       | Sweep pulse time                     |
| acr  | 83e-6      | 8.3E-5     | Initial crater radius        | a      | 1e-6                                    | Initial plasma channel radius        |
| bcr  | 4*Ra       | 2.2E-5     | Initial crater depth         | tus    | 1e-6                                    | US application time                  |
| Ra   | 5.5e-6     | 5.5e-6     | Ra of the processed surface  | pus    | 120[Mpa]                                | Ultrasonic pressure                  |
| rms  | 0.8e-6     | 8.0E-7     | Resolidified material radius | sigmar | 447[Mpa]                                | Static tensile strength SOFT         |
| rbg  | 0.3[mm]    | 3.0E-4 m   | Gas bubble radius            | tau0   | 133.8                                   | Shear fatigue strength SOFT          |

Figure 11. Model parameters System SOFT

(2) The geometry (EDM), time-dependent plasma channel radius - fig. 12); (3) Meshing - fig. 13;

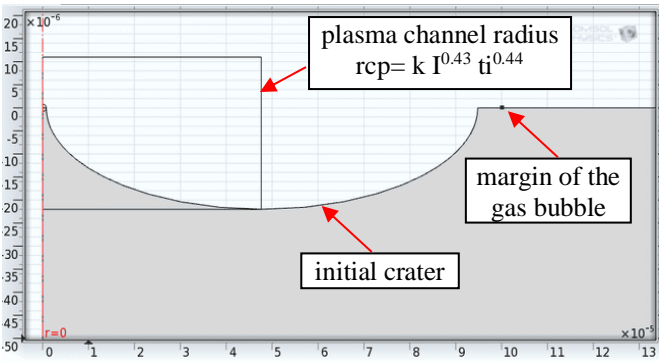


Figure 12. Geometry of the models in the area of interest

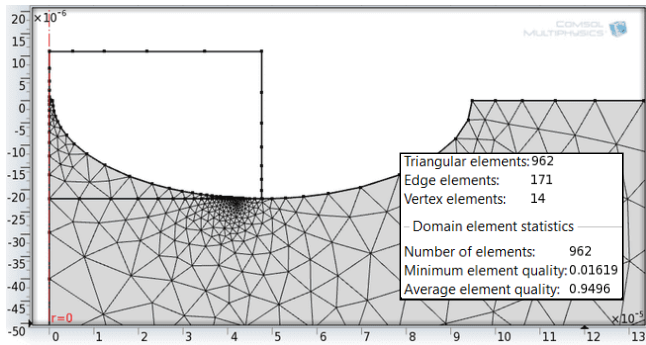


Figure 13. Discretization, statistics and their quality

(4) Introducing material characteristics for System NE alloy - fig. 14 and System Soft - fig. 15;

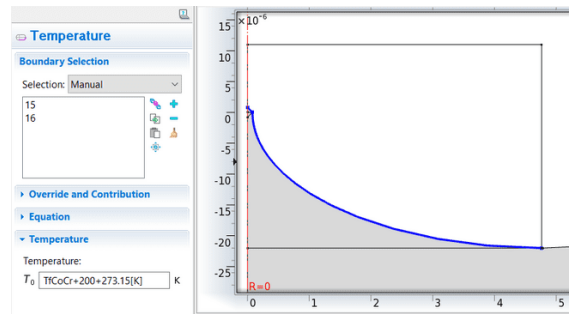
| Property                             | Name | Value    | Unit     |
|--------------------------------------|------|----------|----------|
| ✓ Thermal conductivity               | k    | 14.5     | W/(m*K)  |
| ✓ Density                            | rho  | 8400     | kg/m^3   |
| ✓ Heat capacity at constant pressure | Cp   | 390      | J/(kg*K) |
| ✓ Young's modulus                    | E    | 155[GPa] | Pa       |
| ✓ Poisson's ratio                    | nu   | 0.3      | 1        |

Figure 14. Material characteristics, System NE

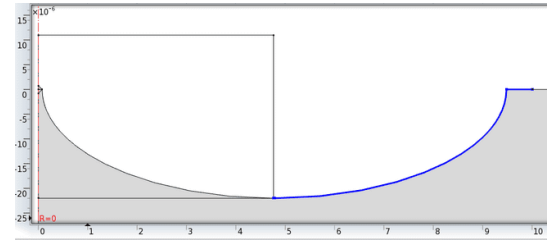
| Property                             | Name | Value    | Unit     |
|--------------------------------------|------|----------|----------|
| ✓ Thermal conductivity               | k    | 13.08    | W/(m*K)  |
| ✓ Density                            | rho  | 8250     | kg/m^3   |
| ✓ Heat capacity at constant pressure | Cp   | 390      | J/(kg*K) |
| ✓ Young's modulus                    | E    | 160[GPa] | Pa       |
| ✓ Poisson's ratio                    | nu   | 0.3      | 1        |

Figure 15. Material characteristics, System SOFT

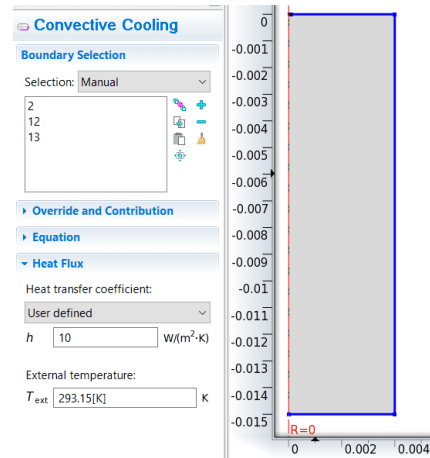
(5) Introducing boundary conditions for the thermal module - fig. 16 and the mechanical module - fig. 17



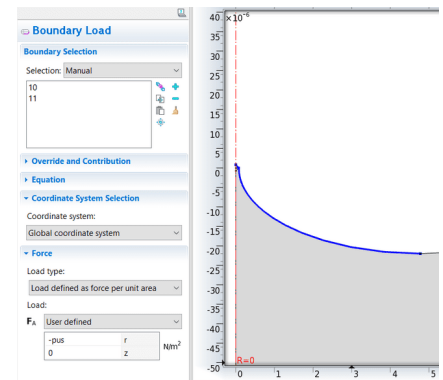
a) temperature at the EDM spot, time-dependent radius



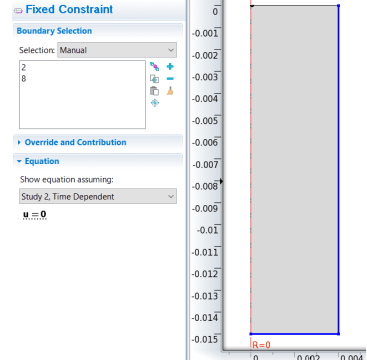
b) thermal insulation produced by the gas bubble



c) convective cooling - workpiece in contact with dielectric  
Figure 16. Boundary conditions - thermal module - EDM



a) cyclic load of the ultrasonic pressure



b) fixed surfaces of the workpiece - holding method

Figure 17. Boundary conditions - mechanical module - US

## 6. NUMERICAL SIMULATION RESULTS

A single discharge was simulated with the thermal module under classical EDM conditions, obtaining the temperature distributions shown in figures 18 and 19. These show the position of the boiling isotherm at the end of the pulse time, which delimits the volume of material removed, according to the overheating model [8]. Values for radius (red arrow) and depth (blue arrow) are validated by real data.

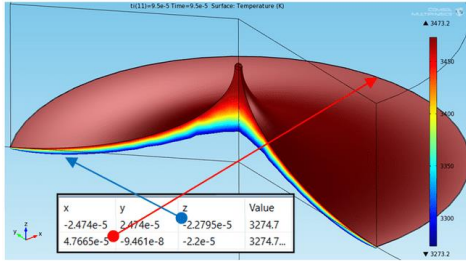


Figure 18. Boiling isotherm at  $t_i=95 \mu s$ , System NE

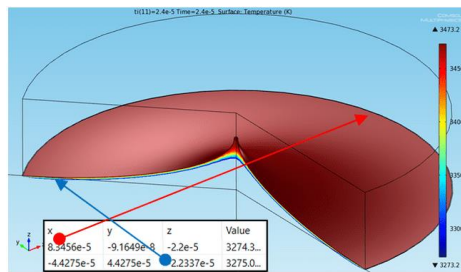


Figure 19. Boiling isotherm at  $t_i=24 \mu s$ , System SOFT

Running the thermal module under EDM+US conditions shows the position of the melting isotherm - fig. 20, 21. The implosion of the gas bubble formed around the plasma channel of the discharge at the end of a US oscillation period allows the dielectric liquid to access the EDM spot area, removing the material delimited by the melting isotherm [8]. Thus, the thickness of the white layer, which comes from the C-enriched melted material of the discharge, becomes much smaller under EDM+US conditions. The probability that the US waves will remove all the melted material is around 30% [8]. For this to happen, the end of the US period ( $T_{us}$ ) must overlap with the duration of the discharge. For the remaining craters where removal occurs through boiling (the discharge does not overlap the end of  $T_{us}$ ), the mechanical material removal happens, caused by the shock waves of the US cavitation, which generate pressures of the order of 100 MPa, acts - fig. 22, 23.

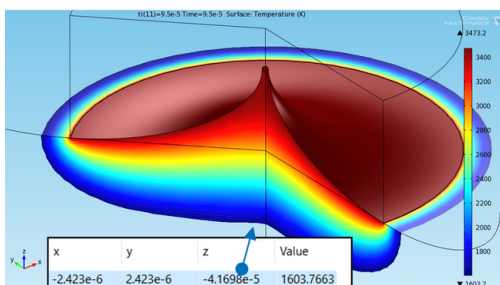


Figure 20. Melting isotherm at  $t_i=95 \mu s$ , System NE

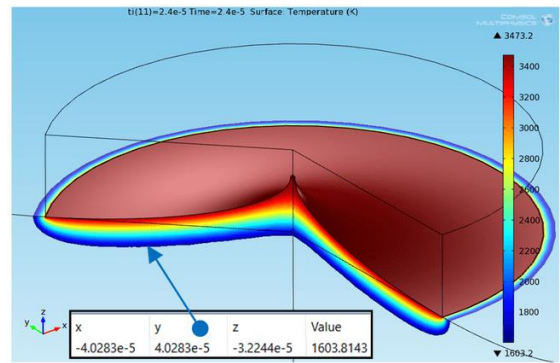


Figure 21. Melting isotherm at  $t_i=24 \mu s$ , System SOFT

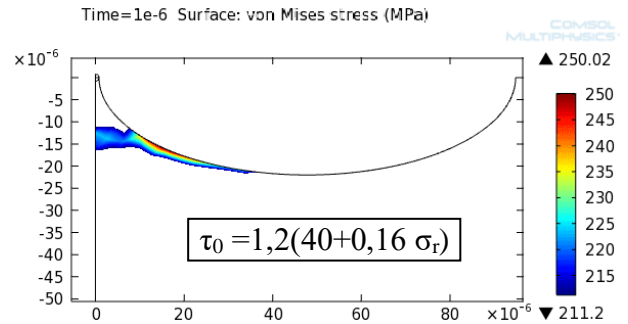


Figure 22. US removal at System NE,  $\tau_0 = 211.2 \text{ MPa}$

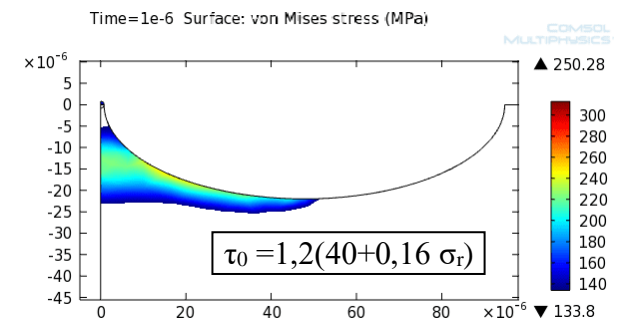


Figure 23. US removal at System SOFT,  $\tau_0 = 133.8 \text{ MPa}$

## 7. ECONOMICAL MODEL FOR EVALUATION OF EDM+US

For choosing the model for determining the cost of the EDM-US hybrid system, several factors were taken into account: the system consists of two large subsystems based on different processing mechanisms, respectively, processing by EDM, and ultrasonic addition; the product is made in small series, even unique in some cases, based on firm order and contract (industrial product); it is first considered the creation of a prototype that will be tested and improved.

Based on these considerations, a mixed method was chosen to calculate the manufacturing cost of the EDM-US hybrid system: in relation to the activities required to manufacture the two subsystems, the ABC (Activity Based Costing) method was chosen, which is based on determining the cost of each group of activities [10]; to determine the cost of each subsystem, the direct cost method was chosen, which is based on the determination of cost components (materials, labour, general expenses, depreciation, etc.).

On this basis, the proposed model for calculating the  $C_T$  total production cost of the EDM-US hybrid system can be determined with the relationship:

$$C_T = C_{EDM} + C_{US} \quad (1)$$

where  $C_T$  = total cost of the system,  $C_{EDM}$  = Cost of EDM subsystem, and  $C_{US}$  = Cost of ultrasonic system. Considering the market of pre-processing equipment through EDM, a maximum selling price of 60000 Euro is proposed, which leads to a maximum production cost of approx. 3878 Euro if we consider VAT of 19% and a profit of 30%.

In order to establish the final selling price under competitive conditions, the Theory of Non-Cooperative Games can be applied which studies and models conflict situations between economic agents [9] and can be applied in cases where the profits (earnings, utility or payments) of each agent economically considered as a market player, they depend not only on their own actions, but also on the actions of other competing firms (players). This theory assumes that players are rational in trying to maximize their profits, using their own interpretations of how other players (firms) will act, and the outcome of the game will ultimately depend on the actions of all players. A fundamental characteristic of non-cooperative games is that it is not possible to sign contracts between players/firms [9] in the legal sense, and cooperation between players appears only as an equilibrium solution.

In the specialized literature [9], it is shown that the theory of non-cooperative games is very useful for modelling and understanding the competition between firms in a certain field characterized by the strategic interdependence of competitors.

Considering the type of product and the study of the main competitors, the hypothesis of applying the theory of non-cooperative games in oligopoly conditions can be accepted, considering a market structure with a relatively small number of firms, in the conditions where none of them can prevent the others from having a significant influence on the market. It is desired to establish the best response of our firm based on the theory of Cournot – Nash equilibrium [9]. Also, this approach is valid in the assumption that our company evolves quickly to become a major player in the market, a very likely scenario considering the market of non-conventional processing, especially in the field of injection mold manufacturing.

The Cournot-Nash model has the following basic characteristics [9]:

**Context:** We consider a market served by  $n$  firms; Homogeneous products - from the point of view of consumers, the goods produced by all companies are perfectly substitutable; Competition by quantity; Simultaneous choice - the  $n$  firms must choose their

outputs simultaneously, respectively each firm must choose its output without knowing the competitors' choices.

**The normal form of the game:**  $i = 1, 2, \dots, n$  (Firms); company outputs  $x_i \geq 0$ , mean  $x_i \in [0, \infty)$ ,  $i = 1, 2, \dots, n$ ; The firm's profit  $i$  (our company) corresponding to the combination of strategies  $(x_i, x_{-i})$  is:

$$\Pi_i(x_i, x_{-i}) = p(x_i + x_{-i}) \cdot x_i - C_i(x_i) \quad (2)$$

where  $\Pi_i(x_i, x_{-i})$  represents the profit of our company,  $p$  – price,  $C_i(x_i) = d + c \cdot x_i$ ,  $d$  – fixed costs,  $c$  – variable costs.

Given the profile of the strategy  $(x_1, x_2, \dots, x_n)$  the relevant point for our company is the total production (total output) made by the other firms:

$$x_{-i} = \sum_{j \neq i} x_j \quad (3)$$

On this basis the strategy profile can be written  $(x_i, x_{-i})$ , and  $\Pi_i(x_i, x_{-i})$  is our firm's profit associated with any combination of strategies in which our firm produces  $x_i$  systems and other firms jointly produce  $x_{-i}$  systems, it being irrelevant for our firm how the total  $x_{-i}$  is distributed among the other  $n-1$  firms.

In Cournot type oligopoly games it is said [9] that  $(x_1^*, x_2^*, \dots, x_n^*) \equiv (x_i^*, x_{-i}^*)$  is a Cournot Nash equilibrium if  $x_i^* = f_i(x_{-i}^*)$ ,  $(\forall) i, i = 1, 2, \dots, n$ , where  $f(x_{-i}^*)$  is the best response function to all the combinations and strategies of the other firms that have the total output  $x_{-i}$ .

To estimate the profit, the reverse demand function is used according to the relationship [9]:

$$p(x) = a - b \cdot x \quad (4)$$

where  $p$  is the price of the product and  $x$  is the number of pieces.

Based on relations (2) and (4) the problem of profit maximization arises:

$$\max_{x_i \geq 0} \Pi_i(x_i, x_{-i}) \equiv [a - b \cdot (x_i + x_{-i})] \cdot x_i - (d + c \cdot x_i) \quad (5)$$

respectively

$$\frac{\partial \Pi_i(x_i, x_{-i})}{\partial x_i} = a - c - 2b x_i - b x_{-i} = 0 \quad (6)$$

and

$$\frac{\partial^2 \Pi_i(x_i, x_{-i})}{\partial x_i^2} = -2b < 0 \quad (7)$$

Based on the Cournot-Nash equilibrium condition it follows

$$x_i = f_i(x_{-i}) = \frac{a - c - b x_{-i}}{2b} \quad (8)$$

Given the non-negativity constraint, or in terms of game theory that the best answer must belong to the player's strategy space, the best answer function for our company is:

$$f_i(x_{-i}) = \max \left\{ \frac{a-c-bx_{-i}}{2b}, 0 \right\} \quad (9)$$

To obtain the equilibrium result, we adopt the alternative "Best response function + Symmetric equilibrium" which assumes that the product is homogeneous, and all firms have the same constant marginal cost,  $c$ . In this case, the Cournot-Nash equilibrium is symmetric  $x_i^* = \bar{x}^*$ ,  $i = 1, 2, \dots, n$  and the following relationship is satisfied [9]:

$$x_i = f_i(x_{-i}), (\forall) i, i = 1, 2, \dots, n \quad (10)$$

In a symmetrical equilibrium  $x_i^* = \bar{x}^*$  and  $x_{-i}^* = (n-1)\bar{x}^*$ ,  $i = 1, 2, \dots, n$ , so that the equilibrium condition becomes:

$$\bar{x}^* = f_i((n-1)\bar{x}^*) = \frac{a-c-b(n-1)\bar{x}^*}{2b} \quad (11)$$

Result

$$x_i^* = \bar{x}^* = \frac{a-b}{b(n+1)} p c s \quad (12)$$

The total equilibrium output will be:

$$x^* = n\bar{x}^* = \frac{n(a-b)}{b(n+1)} b u c \quad (13)$$

Using relation (4) it follows that the Cournot price is:

$$p^* = p(x^*) = \frac{a+nb}{n+1} \text{Euro/pcs} \quad (14)$$

The equilibrium profit will be

$$\Pi_i = \frac{a+nb}{n+1} - c_i \text{Euro/pcs} \quad (15)$$

Using relation (5) or (12)+(14) the total equilibrium profit for firm  $i$  (our firm) can be determined:

$$\Pi_i(x_i, x_{-i}) = \frac{a-b}{b(n+1)} \cdot \left[ \frac{a+nb}{n+1} - c_i \right] \quad (16)$$

Using the relation (16) we can comparatively determine the profit of the firm if it will sell simple and US combined with EDM systems, respectively, depending on the number of competitors which is smaller in the second case.

## 8. CONCLUSIONS

A numerical simulation of the thermal and mechanical material removal during EDM+US was performed, compared to classical EDM, and validated by experimental data. The ability of US to reduce the superficial white layer containing microcracks is highlighted. The reduction is greater in the case of CoCr alloy System SOFT, compared to System NE, due to lower mechanical resistance to cyclic shear stress produced by the ultrasonic cavitation at the end of Tus period. To calculate the cost of manufacturing the EDM-US hybrid system, in relation to the activities required to manufacture the three subsystems, the ABC (Activity Based Costing) method was chosen, which is based on determining the cost of each group of activities and for determining the cost for each subsystem, the direct cost method was chosen, which is based on the determination of cost components (materials, labour,

general expenses, depreciation, etc.). To determine the final sale price under competitive conditions (which in most cases may be different from the previously determined one), Non-Cooperative Game Theory can be applied.

Future research will focus on minimizing the white layer through EDM+US and determining the processing regime, with the key parameter being the ultrasonic pressure (Pus), which is adjusted by the power from the US generator.

## 9. REFERENCES

1. Abu Zeid, O.A. (1997). *On the effect of electro-discharge machining parameters on the fatigue life of AISI D6 tool steel*. J. Mater. Process. Technol., vol. 68, p. 27-32
2. Merdan, M.A.E.R., Arnell, R.D. (1991). *The surface integrity of a die steel after electro-discharge machining, 2. residual stress distribution*. Surf. Eng., vol. 7, p. 154-158.
3. Ghiculescu, D. (2021), "Ultrasonic machining", Course in Romanian, Production Engineering Dept., University Politehnica from Bucharest, Romania.
4. Ghiculescu, D. (2021), „The main technological parameters at EDM”, Course in Romanian, Production Engineering Dept., University Politehnica from Bucharest, Romania.
5. Shabgard, M., Seyedzavvar, M., Oliaei, S. N. B. (2014). „Influence of input parameters on characteristics of EDM process”, University of Tabriz, Tabriz, Iran.
6. Comăneanu, R. M. (2020), “Studies on biomaterials properties, simulations, and applications in dental implantology and prosthesis”, In Romanian, Department of Dental Medicine, University “Titu Maiorescu” from Bucharest, Romania.
7. \*\*\* CoCr Alloys for stomatology, Available at <https://www.dentex.ro/aliaj-co-cr-system-soft-1g>, accessed at: 30.04.2023
8. Ghiculescu, D., *Ultrasonically Aided Electrical Discharge Machining*, in EDM, Types, Technologies and Applications, Nova Publishers, New York, USA, 2015.
9. Aguirre Iñaki, *Notes on Market Power and Strategy*, Department of Economic Analysis, University of the Basque Country, 2020 – 2021, <https://www.ehu.eus/iaguirre/>, accessed 15.05.2023
10. Bâtcă-Dumitru C.G., Sahlian D.N., Şendroiou C., *Managementul performanței - Măsurarea performanței prin metoda Activity Based Costing*, Editura CECCAR, 2019, <https://www.ceccarbusinessmagazine.ro/masurarea-performantei-prin-metoda-activity-based-costing-i-a5784/>, accessed 10.04.2023